J. Environ. Eng. Manage., 19(1), 11-20 (2009)

CHARACTERIZATION OF THE CHANGES IN THE POLARITY AND SIZE OF NATURAL ORGANIC MATTER DURING WATER TREATMENT

Fredrick W. Gerringer,* Fernando L. Rosario-Ortiz and I. H. (Mel) Suffet

Environmental Science and Engineering Program School of Public Health
University of California, Los Angeles (UCLA)
Los Angeles, CA 90095, USA

Key Words: Natural organic matter, polarity, size distribution, conventional filtration, ozone, biofiltration

ABSTRACT

The objective of this research was to evaluate changes to the polarity and size distribution of natural organic matter (NOM) across two water treatment processes: conventional filtration (CF) (coagulation/flocculation, sedimentation, and dual-media filtration) and CF with pre-ozonation and biofiltration (CF-O_3/BF). A variable blend of California State Project water and Colorado River water supplied the treatment trains. NOM polarity and size distribution were measured using the polarity rapid assessment method (PRAM) and ultrafiltration (UF) fractionation, respectively. All polarity and size fractions at each sample location showed temporal variability. Changes in source water blend correlated with changes in NOM polarity, but no relationship was found between the source water blend and NOM size distribution. Both treatment trains decreased NOM hydrophobicity but CF removed more highly charged NOM than CF-O_3/BF. As measured by PRAM, NOM polarity showed less variability after CF-O_3/BF than after CF. The treatment trains had similar effects on the size distribution for the larger size fractions (3-10 kDa and > 10 kDa), but significant differences were measured in the smaller size fractions (< 1 kDa and 1-3 kDa). CF and CF-O_3/BF both reduced the average molecular weight of NOM entering the treatment trains by nearly 20%. Pre-ozonation had little effect on the average molecular weight of NOM in the CF-O_3/BF treatment train. The energy of interaction to molecular weight (ΔE^i/MW) ratio was the same in the pilot plant influent and CF effluent, but CF-O_3/BF lowered this ratio for both the polar and non-polar NOM. This difference was attributed to the pre-ozonation and biofiltration in CF-O_3/BF. These unit processes decreased ΔE^i in non-polar and polar NOM, leading to the lower ΔE^i/MW ratios. Results from this research clearly indicate PRAM and UF fractionation can detect NOM changes during water treatment.

INTRODUCTION

Natural organic matter (NOM) is a mixture of organic molecules derived from decomposing living matter and from biological activity within water bodies [1,2]. These compounds are classified into humic materials such as humin, humic acids, and fulvic acids and non-humic materials such as proteins, amino acids, sugars, and polysaccharides [1-3]. The importance of NOM is demonstrated by its role in disinfection by-product (DBP) formation [4-6], membrane fouling [7-9], and coagulation [10,11]. Consequently, the transformations of NOM caused by water treatment processes have been of significant interest [12-14].

Molecular weight (MW), or size, distribution, and polarity are two important parameters for characterizing NOM [15-17]. NOM size distribution can be evaluated with several methods, of which ultrafiltration (UF) fractionation [18-21] is one of the most common. NOM polarity is frequently measured according to the XAD resin method [22], which separates fractions based on their successive affinity toward resins with different polarities. However, this method is conducted at low pH and has other limitations such as large sample volumes and long processing times that limit its usefulness for frequent monitoring. As a result, an alternate polarity characterization method has been developed to reduce the sample volume and analytical time, therefore allowing the characterization of the polarity for numerous samples

*Corresponding author
Email: fgerringer@mwdh2o.com

[23-25].

Research has shown water treatment processes modify NOM polarity and size distribution. For example, ozonation transforms hydrophobic compounds into hydrophilic compounds [26-28] and lowers the average MW of NOM [26,28]. Ozonation also forms biodegradable dissolved organic matter (BDOM), including aldehydes, ketoacids and carboxylic acids [29,30]. Subsequent biofiltration can remove this BDOM with efficiencies greater than 70% when using granular activate carbon biological filters [29]. Studies have shown coagulation preferentially removes NOM that is larger [28,31,32] and more humic (i.e., hydrophobic) in nature [28].

The objective of this study was to understand and compare the changes in NOM polarity and size distribution during conventional filtration (CF) (coagulation/flocculation, sedimentation, and dual-media filtration) and CF with pre-ozonation and biofiltration (CF-O_3/BF). The polarity rapid assessment method (PRAM) [23-25] was selected to characterize NOM polarity because it quickly processes small sample volumes at ambient pH. NOM size distribution was evaluated using UF fractionation also conducted at ambient pH. Once these changes are better understood, future research can explore the possibility of using these parameters to optimize the performance of water treatment processes.

METHODS

1. Pilot Plant

This research used a dual-train pilot plant with a flow rate of 17 L min^{-1} per train to treat raw water using CF and CF-O_3/BF (Fig. 1) at the Metropolitan Water District of Southern California's (MWDSC) research facility in La Verne, California. The influent was a blend of Colorado River water (CRW) and California State Project water (SPW) controlled by the operational needs of the full-scale treatment plant at the same location.

Coagulation was achieved using 2.5 mg L^{-1} aluminum chlorohydrate (ACH) (Sumalchlor 50, Summit Research Labs, Flemington, NJ) and 2.0 mg L^{-1} cationic polymer (polydimethyldiallyl ammonium chloride, NS 3150, Neo Solutions, Inc., Beaver, PA). Sodium hypochlorite added to the rapid mix of the CF process maintained a free chlorine residual of 1.5 to 2.5 mg L^{-1} (Hach Company CL-17 chlorine analyzer, Loveland, CO). at the filter effluent. Ammonium sulfate (AM185, Spectrum Chemicals & Laboratory Products, Gardena, CA) was added at the filter effluent to convert the free chlorine to chloramines (3:1 chlorine to ammonia w/w ratio).

For CF-O_3/BF, an air-fed ozone generator (Trailigaz Labo, Trailigaz Ozone of America, Inc., Jenkintown, PA) applied a dose of 1.0 mg O_3 L^{-1} of

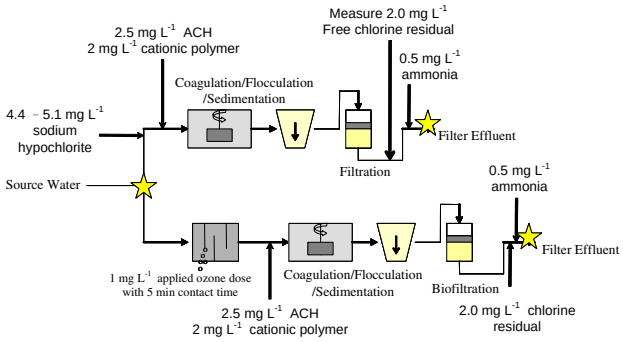

Fig. 1. Process diagram for CF (top) and CF-O_3/BF (bottom). The stars indicate water quality and NOM sample collection sites.

water through two diffusers at the bottom of separate 15 cm diameter, 6.1 m tall glass columns with a downward water flow of 9.5 L min^{-1}. Each contactor was followed by a second column to provide a total contact time of 5 min. Sodium hypochlorite and ammonium sulfate were added to the CF-O_3/BF effluent to maintain a chloramine residual of 1.5-2.5 mg L^{-1}.

The filters contained 51 cm of anthracite coal and 20 cm of sand and had filtration rate of 1.8 L min^{-1} m^{-2}. Backwashs were based on the following criteria: (1) effluent turbidity (Hach 2100N Turbidimeter, Hach Company, Loveland, CO) exceeding 0.3 NTU; (2) headloss greater than 1.8 m, or (3) filter runs longer than 24 h.

Samples were collected at the pilot plant influent, the ozone contactor effluent, and the process effluent of each treatment train during November and December of 2003. Weekly water quality grab samples and bi-weekly NOM grab samples were collected from the locations shown in Fig. 1. Water quality samples were analyzed according to Standard Methods [33].

2. Polarity Characterization

PRAM, which has been described in detail elsewhere [23-25], uses the non-polar (C-18 and C-2), polar (CN, Diol, and Silica), and anion exchange (NH-2 and SAX) solid-phase extraction (SPE) cartridges (Alltech Associates, Deerfield, IL). These cartridges were cleaned by flushing with Milli-Q to minimize ultraviolet absorption at 254 nm (UV_{254}). Water samples were run (Varian Instruments, Walnut Creek, CA) with a 1 cm path length, micro-flow cell (Fisher Scientific, Pittsburgh, PA) to create an UV_{254} breakthrough curve. A syringe pump (KD Scientific Model 100, Holliston, MA) maintained a flow of 1.2 mL min^{-1} through all of the cartridges except CN, which had a flow of 1.67 mL min^{-1}.

Results from PRAM experiments were compared using the retention coefficient (RC), which measures NOM polarity by describing the fraction of UV absorbing material retained within each cartridge. The

equation used to calculate this quantity was RC = 1 – A/A_0, where A was the average maximum UV_{254} for each breakthrough curve and A_0 was the UV_{254} of the initial sample. The value for A was obtained by averaging the UV_{254} values after a constant breakthrough level had been achieved. Each resin produced a separate RC value because the resins interacted with different NOM polarity fractions [23-25].

3. Size Distribution

UV_{254} also was used to evaluate NOM size fractions produced by parallel UF fractionation. This method used a 76 mm inside diameter, 400 mL Teflon-lined stainless steel cell with a magnetic stir bar (Amicon, Inc.; Beverly, MA) pressurized to 240 kPa with nitrogen gas. The UF membranes (Amicon YM 1, YM 3, and YM 10; Amicon, Inc., Beverly, MA) had nominal MW cutoffs of 1, 3, and 10 kDa, respectively.

To minimize leaching of UV absorbing material, the manufacturer recommended pretreatment for the membranes. The UF membranes were soaked in a 5% NaCl solution for at least 30 min before soaking for a minimum of 15 min in four consecutive baths of deionized (DI) water (Milli-Q Plus water system, ZD 40 115 95, Millipore Corp., Bedford, MA). The final step was to rinse the membranes with 100 mL DI water before beginning filtration.

Each experiment began by filtering a 100 mL DI water blank to quantify the amount of UV_{254} absorbing material leaching off the UF membrane. Next, 200 mL of sample was added to the UF cell for fractionation and an aliquot of the bulk sample was collected to measure A_0. To minimize breakthrough, fractionation was stopped once the membrane filtered 100 mL of sample. The filtrate and the water remaining in the UF cell, called the retentate, were collected for UV_{254} measurement. Each membrane was discarded after one use.

This method separated the NOM samples into the following size fractions: < 10 kDa, < 3 kDa, and < 1 kDa. Using the equations below produced the NOM size distribution for the samples:

$$A_0 - < 10 \text{ kDa} = < 10 \text{ kDa} \quad (1)$$

$$< 10 - < 3 \text{ kDa} = 3\text{-}10 \text{ kDa} \quad (2)$$

$$< 3 - < 1 \text{ kDa} = 1\text{-}3 \text{ kDa} \quad (3)$$

$$< 1 \text{ kDa} = < 1 \text{ kDa} \quad (4)$$

The right sides of the above equations indicate the size fractions used for this analysis. The final step involved dividing the UV_{254} for each size fraction by the total influent UV_{254} collected on the same day to produce the normalized size fraction data. Due to UV_{254} reduction during treatment, the sum of these ratios for the process effluents was less than one.

Other fractions considered for analysis were > 100 kDa, 10-100 kDa, 5-10 kDa, and 3-5 kDa. However, adding more size fractions would reduce the ability to detect significant differences between those fractions because the pilot plant influent had low total UV_{254} relative to the standard error for the fractionation experiments. Additionally, the > 100 kDa fraction was zero or nearly zero for all samples and the CF effluent for 11/19/2003 was not fractionated using a 5 kDa membrane because not enough sample was available. For these reasons, the researchers focused on the size fractions shown in Eqs. 1-4.

4. Energy of Interaction to MW Ratio Calculation

In order to further evaluate the effect of treatment on the physicochemical properties of NOM, the energy of interaction to MW (ΔE^i/MW) ratio was estimated. The average MW for each sample location was determined by considering the proportional contributions of the different size fractions. To calculate this quantity, the UV_{254} of a size fraction was multiplied by the average MW of the range of that fraction and divided it by the total UV_{254} of that sample. The average MW of the largest fraction (> 10 kDa) was estimated at 10 kDa because the upper boundary of that fraction is undefined. Adding the results of each size fraction for a sample together provided an estimate of the average MW of the NOM in UV equivalents.

The energy of interaction of the NOM was estimated from the interaction between NOM and the SPE sorbents used for PRAM analysis. This interaction is dependent upon the affinity between specific portions of the NOM and the sorbents. For example, the hydrophobic moieties of the C-18 sorbent and the hydrophilic moieties measured by the Diol sorbent will interact with similar moieties in NOM molecules. One way to describe the energy of interaction between NOM and the SPE sorbents is by calculating the solubility parameter (δ), defined by Eq. 5, for the sorbents used:

$$\delta = \left(\frac{\Delta E^v}{V_m} \right)^{1/2} \quad (5)$$

In this expression, ΔE^v is the energy of vaporization and V_m is the molar volume [34]. The interaction between NOM and a specific SPE sorbent (i.e., C-18) will depend on the similarity of δ for the NOM and C-18 species. Therefore, it could be assumed the calculated δ for a given SPE sorbent would be similar to the value expected for a specific fraction of the NOM.

An estimated value for ΔE^i between NOM and a particular SPE sorbent could be obtained using Eq. 6.

$$\Delta E^i = \delta^2 \times V_m \quad (6)$$

If ΔE^i is assumed to be equal to ΔE^v for an interacting NOM moiety, Dividing ΔE^i (J) by the average MW (Da) produces a ΔE^i/MW ratio. For this analysis, non-

Table 1. Water quality data for NOM grab samples

Sample Date and Location	% SPW[a]	TOC (mg L^{-1})	UV_{254} (cm^{-1})	SUVA (L mg^{-1})	TDS (mg L^{-1})
11/19/2003					
Influent	76	2.5	0.058	2.32	345
CF Effluent	76	2.0	0.042	2.10	360
CF-O_3/BF Effluent	76	2.0	0.037	1.85	350
12/4/2003					
Influent	80	2.5	0.059	2.36	331
CF Effluent	80	2.1	0.048	2.29	344
CF-O_3/BF Effluent	80	2.1	0.035	1.67	340
12/16/2003					
Influent	92	2.6	0.067	2.58	298
CF Effluent	92	2.1	0.049	2.33	310
CF-O_3/BF Effluent	92	2.0	0.047	2.35	309

[a]The remaining water comes from the Colorado River.

polar and polar components of NOM were approximated by the C-18 and Diol sorbents, respectively. V_m and δ for these sorbents were calculated using Molecular Modeling Pro (version 5.1.8, Fairfield, CA). The structure of each compound was minimized prior to calculation.

RESULTS AND DISCUSSION

1. Water Quality Data

Table 1 presents the CRW and SPW blends and water quality data for the influent and process effluents on the sample collection dates. The influent water pH was 8.1 and the applied ozone dose in the CF-O_3/BF train was calculated to be 1.1-1.2 mg L^{-1} on the days of NOM sample collection. Both treatment trains removed approximately 20% of TOC, but CF-O_3/BF reduced UV_{254} by 35% whereas CF only lowered it about 25%. Larger declines of UV_{254} than TOC indicates these treatment trains modified or removed aromatic NOM more easily than other NOM components. The specific UV absorbance (SUVA), which correlates with percent aromaticity [35], declined 20% during CF-O_3/BF and less than 10% during CF. These data showed CF-O_3/BF more effectively reduced NOM aromaticity through the ozonation of aromatic functional groups.

2. Polarity Analysis

PRAM data for the influent, CF effluent, and CF-O_3/BF effluent are shown in Fig. 2. The error bars represent the standard error as determined using propagation of error analysis [36]. While the results described here refer to the portion of NOM that absorbs UV light at 254 nm, other research has shown RC values based on TOC and UV_{254} to be similar [25]. These data cannot be compared to polarity characterization using XAD resins because PRAM analyzes polarity at ambient pH and does not attempt to physically separate NOM with different polarities [23].

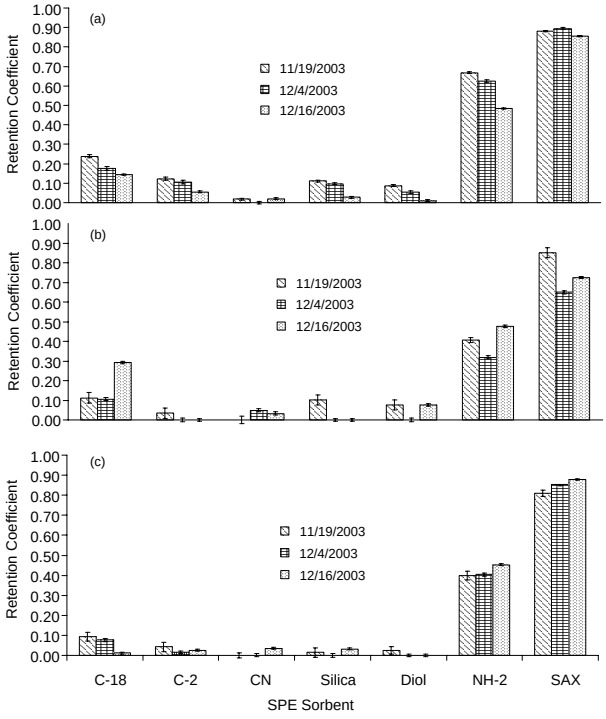

Fig. 2. RCs for the (a) pilot plant influent, (b) CF effluent and (c) CF-O_3/BF effluent.

Figure 2a presents the RCs for the shared influent to both treatment trains and demonstrates the variable nature of the NOM entering the pilot facility. The RCs ranged from 0.50-0.90 for the anion exchange resins (NH-2 and SAX), 0.00-0.10 for the polar resins (CN, Silica, and Diol) and 0.05-0.25 for the non-polar resins (C-18 and C-2). Negative charges associated with NOM at a pH of 8.0-8.2 (e.g., carboxylic groups) caused the high RCs observed for the anion exchange sorbents. RCs for C-18 and C-2 were 0.15-0.25 and 0.05-0.12, respectively, and are positively correlated to the availability of hydrophobic surface area [23]. The polar resins, Silica and Diol, have RCs of less than 0.10, indicating the NOM had low uncharged po-

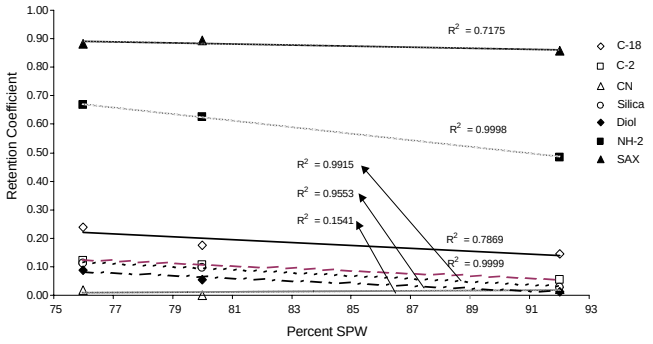

Fig. 3. Linear regressions showing the relationship between RC and the percent SPW in the influent water. R^2 values closer to 1.0 indicate variability in the percentage of SPW better explains the RC variability for a particular resin.

larity. However, the results for Silica and Diol may cause the NOM polar fraction to be underreported because water can decrease the apparent interaction between these resins and NOM by saturating the active sites on the resins. Higher blends of SPW lowered the polarity response between the NOM and all the resins except SAX and CN, which was near zero for all three samples. As shown by the linear regressions in Fig. 3, the variability detected in the influent NOM samples was mostly explained by the proportion of SPW in the raw water.

After CF, the RCs were 0.30-0.85 for the anion exchange resins, 0.00-0.10 for the polar resins, 0.00-0.30 for the non-polar resins (Fig. 2b). The ranges of these values are similar to those of the influent, although significant differences were measured between the influent and effluent samples from the same date. With the exception of the RC for C-18 from the last sample date, CF reduced NOM hydrophobicity. This result is similar to what has been seen after coagulation [28] and is not surprising since sedimentation is a physical process unlikely to affect polarity and filtration has little effect on NOM characteristics [37]. Lower RC values for the anion exchangers, particularly for the weak anion exchanger (NH-2), show charge neutralization from coagulation decreased the overall charge of the NOM. The three samples varied significantly from each other and showed no evidence of the influent polarity trends.

RC data for the CF-O_3/BF effluent were 0.00-0.10 for the polar and non-polar SPE sorbents and 0.40-0.88 for the anion exchange sorbents (Fig. 2c). Since ozonation transforms hydrophobic NOM to hydrophilic NOM [26-28], the low RC values for the hydrophobic resins were expected. Data for the polar resins were near zero and generally lower than the influent samples, showing polar NOM produced during ozonation were subsequently removed. As expected, CF-O_3/BF reduced the RCs for NH-2 but only had a minimal effect on the data for SAX, revealing some decrease in the overall NOM charge. Results for CF-O_3/BF demonstrated limited variability between the three samples, indicating this process produced NOM with relatively consistent polarity in spite of changes to the source water blend.

PRAM data collected during this research show the CF and CF-O_3/BF processes had different effects on NOM polarity. While changes to the NH-2 RCs were similar between these processes, CF also significantly reduced the SAX RCs. These data indicate CF was more effective at reducing the overall charge on the NOM. The data from the polar resins were mixed, with RCs for CF-O_3/BF typically equal to or lower than those for CF. Except for the C-18 RC from 12/16/2003, both treatment trains showed comparable reductions in the RCs for the hydrophobic resins. Overall, CF-O_3/BF produced NOM with more consistent polarity characteristics than CF. The probable causes of these differences are the different unit operations included in these processes (e.g., prechlorination versus pre-ozonation), inconsistent treatment train performance, and variable reactivity of the influent NOM.

3. Changes in Size Distribution

The normalized influent size distribution data are shown in Fig. 4a with error bars representing the standard error of each fraction calculated by the propagation of error method [36] and divided by the corresponding total influent UV_{254}. Temporal variability was detected in the total influent UV_{254} (Table 1) and the NOM size fractions (Fig. 4a). The largest UV_{254} fraction switched from < 1 to 3-10 to 1-3 kDa during the course of testing, although the 1-3 kDa fraction was not statistically larger than the next largest fraction from that day. Except for the > 10 kDa fraction from the second sample, the other size fractions showed they contained similar amounts of NOM. R^2 values from linear regression (data not shown) indicated the source water blend did not explain NOM variability for size distribution as well as it did for NOM polarity.

Size fraction data for CF effluent are displayed in Fig. 4b. Table 1 shows UV_{254} removal varied from 20-30%, with the lowest removal on 12/4/2003. The > 10 , 3-10, and 1-3 kDa fractions showed no significant changes in CF effluent UV_{254} over time. Other research has documented significant reductions in the > 10 kDa fraction after CF [38], but in that instance the > 10 kDa fraction composed nearly 70% of the influent NOM. Only 10-20% of the influent NOM was found in that fraction during this research, thus there were not as many large organics to remove. NOM size distribution showed less variability in the CF effluent than the influent, suggesting the process stabilized these NOM size fractions.

Figure. 4c shows the NOM size distribution after

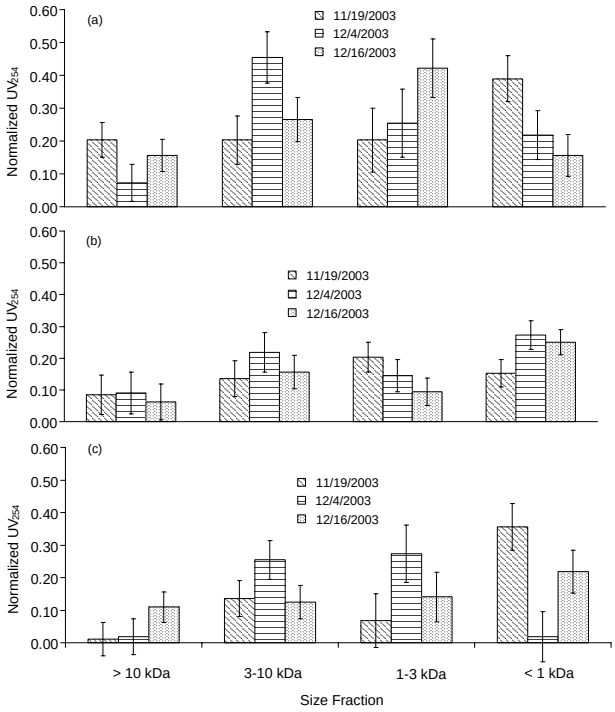

Fig. 4. NOM size fraction data for (a) pilot plant influent, (b) CF effluent, and (c) CF-O_3/BF effluent normalized by the total influent UV_{254} for each sample date. Total CF effluent UV_{254} declined by 0.025 cm^{-1}, 0.015 cm^{-1}, and 0.028 cm^{-1} on 11/19/2003, 12/4/2003, and 12/16/2003, respectively. Total CF-O_3/BF effluent UV_{254} declined by 0.025 cm^{-1}, 0.024 cm^{-1}, and 0.026 cm^{-1} on those sample dates, respectively.

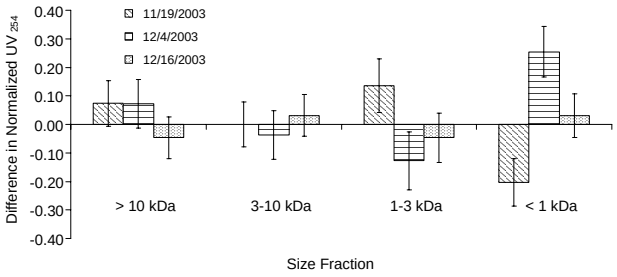

Fig. 5. Normalized size fraction data for CF-O_3/BF effluent subtracted from CF effluent. Positive values indicate the CF effluent had a higher UV_{254} for a particular fraction than CF-O_3/BF effluent. The opposite is true for negative values.

CF-O_3/BF, a process expected to remove large MW organics through ozonation [26,28] and coagulation [28,31,32]. While UV_{254} removal was 30-40%, none of the size fractions was significantly removed from all three samples. However, UF fractionation did detect temporal variability in the > 1, 1-3, and 3-10 kDa fraction as well as with the overall size distribution. For example, the < 1 kDa fraction had the highest UV_{254} in the first sample, but the UV_{254} of all the fractions had overlapping error bars in the last sample. The low UV_{254} in the influent > 10 kDa fraction probably contributed to the minimal removal of UV_{254} from that fraction during CF-O_3/BF. The pre-ozonation unit process had little effect on the average MW of the NOM (Table 2) even though other research has shown ozone to decrease the MW of NOM [26,28]. This result may be a consequence of the low amount of the largest size fraction (> 10 kDa) in the influent water compared to research using other source waters [38].

The difference in UV_{254} between the four size fractions for the CF and CF-O_3/BF effluents is shown in Fig. 5. To create this graph, CF-O_3/BF effluent data were subtracted from CF effluent data. Positive values indicate the CF effluent had a higher UV_{254} for a particular fraction and negative values indicate the opposite. These data showed no significant difference between the treatment processes when the error bars cross the x-axis.

UF fractionation detected no significant differences between the > 10 and 3-10 kDa fractions, indicating CF and CF-O_3/BF changed these fractions similarly. The < 1 and 1-3 kDa fractions showed significant differences between the processes on 11/19/2003 and 12/4/2003, demonstrating NOM with a lower MW had more variability than larger NOM. The third data set, which corresponded with the highest blend of SPW, was the one sample without any significant differences between CF and CF-O_3/BF. These data might indicate high SPW blends (> 90%) reduce the differences in NOM size distribution after these treatment processes. As with the polarity data, the variability detected by this analysis was probably caused by a combination of the different unit operations for each train,

Table 2. Average MW and ΔE^i data for the three NOM samples dates. These data were used to calculate the ΔE^i/MW ratios shown on the right. The errors for the ΔE^i/MW ratios were determined using the standard errors of the RC and UF data

NOM Sample Location	Average MW (kDa)	ΔE^i (J)		ΔE^i/MW Ratio (J Da^{-1})	
		Non-Polar	Polar	Non-Polar	Polar
Influent	4.2	9200	2200	2.2 ± 0.5	0.52 ± 0.13
CF Effluent	3.4	8500	2200	2.5 ± 1.0	0.65 ± 0.32
Ozone Effluent	4.1	7300	5800	1.8 ± 0.6	1.4 ± 0.5
CF-O_3/BF Effluent	3.5	3000	350	0.86 ± 0.39	0.10 ± 0.16

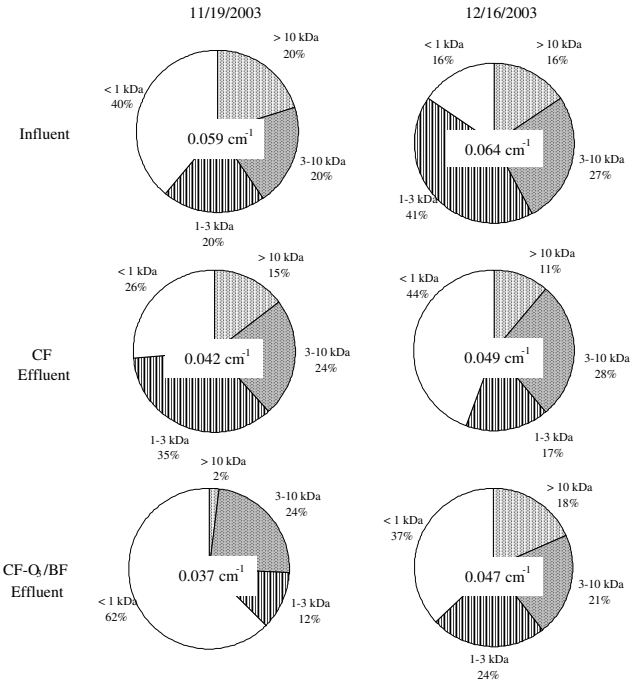

Fig. 6. Pie charts for two sample dates show temporal differences in the influent UV_{254} size distribution and how the CF-O_3/BF and CF treatment trains changed the size distribution. The sample dates are included at the top of the graphs and the sample sites are listed to the left. Results are shown as a percentage of the total UV_{254} (shown in the center of each pie chart) for the given sample site on the indicated date.

inconsistent process performance, and variable reactivity of the influent NOM.

Another approach to analyzing the size distribution involves pie charts showing the percentage of UV_{254} measured in the size fractions. Figure 6 shows these data for influent, CF effluent and CF-O_3/BF effluent samples from 11/19/2003 and 12/16/2003 to demonstrate how the size distribution can change over time and with treatment. Unlike the bar graphs in Figs. 4b and 4c, this analysis normalizes the size fraction data of a sample by its total UV_{254} instead of the influent UV_{254} to present the results from a different perspective. The center of each pie chart displays the total UV_{254} for that sample. The top two pie charts contain the same data for the 11/19/2003 and 12/16/2003 influent samples shown in Fig. 4a but were included for comparison with CF effluent and CF-O_3/BF effluent results.

The two middle pie charts in Fig. 6 indicate CF caused minor changes in the percentage of UV_{254} in the 3-10 and > 10 kDa fractions of both samples. The percentage of UV_{254} in the < 1 kDa fraction decreased on 11/19/2003 but increased on 12/16/2003. The opposite effect of nearly the same magnitude was seen for the 1-3 kDa fraction. Combining results for the

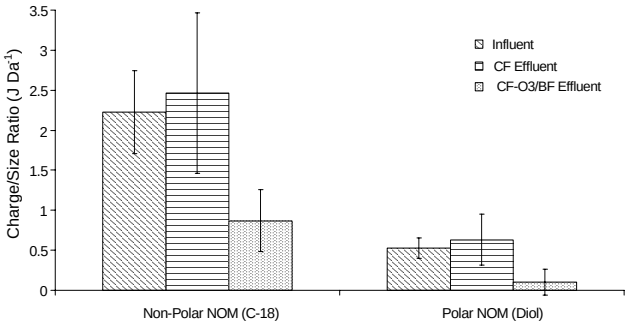

Fig. 7. Average ΔE^i/MW ratio in terms of ΔE^i (J) and MW (Da) for non-polar and polar NOM at the pilot plant influent and the effluent of each treatment train. The Hansen solubility parameter for C-18 and Diol SPE resins were used to determine the ΔE^i/MW ratio of the non-polar and polar components of the NOM, respectively. Error bars represent the standard error for these data.

smaller two size fractions shows NOM with a MW of less than 3 kDa composed approximately 60% of the UV_{254} before and after the CF treatment train. A similar analysis of the 12/4/2003 influent data in Fig. 4a reveals 50% of the UV_{254} was in the smaller two size fractions, although the CF effluent still had 60% of the UV_{254} in those size fractions (data not shown).

The two bottom pie charts in Fig. 6 show the percentage of UV_{254} in the < 1 kDa size fraction increased after CF-O_3/BF. However, the distribution of UV_{254} for these samples showed more variability than after CF treatment. For example, the amount of UV_{254} in the smaller two size fractions of the CF-O_3/BF effluent was 70, 50, and 60% for the 11/19/2003, 12/4/2003 (data not shown), and 12/16/2003 samples, respectively. Also, UV_{254} was relatively evenly distributed on 12/16/2003 compared to 11/19/2003, which had more than 60% in the < 1 kDa fraction and almost nothing in the > 10 kDa fraction.

4. ΔE^i/MW Ratio

The average non-polar and polar ΔE^i/MW ratios (J Da^{-1}) for each sample site are shown in Fig. 7. PRAM data from the C-18 and Diol sorbents were used to calculate the ΔE^i/MW ratio for the non-polar and polar NOM, respectively. Comparisons between ΔE^i/MW ratios are appropriate only between values calculated using the same sorbent. One reason for this limitation is the difficulty NOM has displacing water from the saturated active sites of the Diol sorbent, which lowers the RC value and the calculated ΔE^i of the polar NOM. Since the C-18 sorbent does not experience the same phenomenon, the ΔE^i of the non-polar NOM will be relatively higher than the ΔE^i of the polar NOM, which affects comparisons between

their respective ΔE^i/MW ratios.

A comparison of the influent and CF effluent data (Fig. 7) shows the CF treatment train did not change the ΔE^i/MW ratio for either the non-polar or polar NOM. However, the CF-O_3/BF treatment train significantly decreased the ΔE^i/MW ratio for both the non-polar and polar NOM. Examining the data used to calculate the ΔE^i/MW ratio showed that both treatment trains decreased the average MW of the NOM by nearly 20% (Table 2). Therefore, the observed differences between ΔE^i/MW ratios after CF and CF-O_3/BF were caused by the dissimilar effects of these treatment trains on ΔE^i of the NOM (Table 2). CF decreased ΔE^i of the non-polar NOM by less than 10% and did not change ΔE^i of the polar NOM. The 70-80% declines in ΔE^i of the non-polar and polar NOM during CF-O_3/BF treatment resulted in significantly lower ΔE^i/MW ratios than those in the CF effluent (Table 2).

The combined effect of pre-ozonation and biofiltration was likely responsible for the observed differences between the treatment trains. Table 2 also shows average MW, ΔE^i, and ΔE^i/MW ratio data for NOM for the ozonation effluent. These data show ozonation decreased ΔE^i of the non-polar NOM by approximately 20% while increasing ΔE^i of the polar NOM by more than 250%. The lower ΔE^i for the non-polar NOM was probably caused by ozonation transforming non-polar NOM into polar NOM and decreasing the RC value used in the NOM ΔE^i calculations. However, between the ozone contactor effluent and CF-O_3/BF effluent, ΔE^i of the non-polar NOM decreased by 50% and the polar NOM decreased by 90%. The unit processes between those sample locations included coagulation/flocculation, sedimentation, and biofiltration. Since coagulation/flocculation and sedimentation were common to the CF and CF-O_3/BF treatment trains, it is unlikely these unit processes accounted for the declines in ΔE^i seen between the ozone contactor and CF-O_3/BF effluents. Therefore, it is hypothesized the decline in the ΔE^i/MW ratio of NOM, particularly for the polar NOM, was primarily caused by the biofilter of the CF-O_3/BF treatment train.

CONCLUSIONS

This research compared changes to NOM polarity and size distribution during CF-O_3/BF and CF trains. All polarity and size fractions at each sample location showed temporal variability. Polarity data demonstrated the influent NOM was highly charged with some hydrophobic regions available to interact with non-polar compounds. Influent NOM polarity depended primarily on the source water blend, with SPW having a lower affinity for the C-18, C-2, Silica, Diol, and NH-2 resins than CRW. Variability in the influent size fraction data did not change consistently with higher SPW blends. These findings reveal changes to the source water blend correlated with changes to NOM polarity but not with changes to NOM size distribution.

As expected, the CF-O_3/BF and CF trains decreased hydrophobicity, but CF-O_3/BF produced NOM with more consistent polarity. While both treatment trains removed significant amounts of the highly charged NOM, CF did so more efficiently. The polarity response to the C-18, NH-2, and SAX resins after CF-O_3/BF changed consistently with the percentage of SPW, showing some polarity differences in the process influent were detected in the effluent.

Size distribution analysis showed the influent NOM size distribution was unrecognizable in the effluents of both treatment trains. However, CF was found to reduce differences between the size fractions more than CF-O_3/BF. The low amount of NOM in the largest size fractions caused the removal of that fraction to be lower than expected. Both treatment trains has similar effects on the size distribution for the larger fractions (3-10 and > 10 kDa), but significant differences were measured in the smaller fractions (< 1 and 1-3 kDa).

The ΔE^i/MW ratio data highlighted how the treatment trains affected the relationship between NOM ΔE^i and MW. CF and CF-O_3/BF caused similar declines in the average MW of NOM, but CF-O_3/BF caused much larger decreases in ΔE^i of non-polar and polar NOM. Pre-ozonation was found to decrease ΔE^i of non-polar NOM and increase ΔE^i of polar NOM. Subsequent biofiltration in CF-O_3/BF was hypothesized to decrease ΔE^i in non-polar and polar NOM, leading to the lower ΔE^i/MW ratios in the effluent of this treatment train.

These results clearly show PRAM and UF fractionation can detect changes to NOM polarity and size distribution during water treatment. Future research should use one water source so variability attributed to natural fluctuations in that source water can be readily identified. The UF fractionation method used for this research should be further refined to provide more precision when analyzing water with low total UV_{254}. Otherwise, the large error bars make it difficult to discern differences between size fractions. Additional studies are needed to explore the relationship between NOM characteristics and water treatment endpoints that are important to water utilities, such as finished water turbidity, DBP formation, and the minimization of fouling in downstream membranes. Once these relationships are defined, evaluating NOM polarity and size distribution as described in this research may be useful as a process design or monitoring tool to assist with regulatory compliance.

ACKNOWLEDGEMENTS

Funding for this project was provided by the

California Department of Water Resources and MWDSC. The authors would like to acknowledge the following individuals for their contributions: Dr. Christopher Gabelich of MWDSC for his invaluable guidance during every phase of this research; Hakam Al-Samarrai, Po Fung, and Susan Givens (all formerly of UCLA) for conducting the UF fractionation experiments; and Jerry Pitts (formerly of MWDSC), Ray Evangelista, and Minhaal Kalyan (both formerly of California State Polytechnic University, Pomona) for assisting with the operation and maintenance of the pilot plant.

REFERENCES

1. Stevenson, F.J., Humus Chemistry, Genesis, Composition, Reaction. 2nd Edition, John Wiley & Sons, New York (1994).
2. Thurman, E.M., Developments in Biochemistry: Organic Geochemistry of Natural Waters. Nijhoff & Junk Publishers., Dordrecht, The Netherlands (1985).
3. Krasner, S.W., J.P. Croué, J. Buffle and E.M. Perdue, Three approaches for characterizing NOM. J. Am. Water Works Ass., 88(6), 66-79 (1996).
4. Amy, G.L., J.M. Thompson, L. Tan, M.K. Davis and S.W. Krasner, Evaluation of THM precursor contributions from agriculture drains. J. Am. Water Works Ass., 82(1), 57-64 (1990).
5. Zhang, X.G. and R.A. Minear, Characterization of high molecular weight disinfection byproducts resulting from chlorination of aquatic humic substances. Environ. Sci. Technol., 36(19), 4033-4038 (2002).
6. Singer, P.C., Humic substances as precursors for potentially harmful disinfection by-products. Water Sci. Technol., 40(9), 25-30 (1999).
7. Lee, N., G. Amy, J. Croué and H. Buisson, Identification and understanding of fouling in low-pressure membrane (MF/UF) filtration by natural organic matter (NOM). Water Res., 38(20), 4511-4523 (2004).
8. Taniguchi, M., J.E. Kilduff and G. Belfort, Modes of natural organic matter fouling during ultrafiltration. Environ. Sci. Technol., 37(8), 1676-1683 (2003).
9. Amy, G. and J. Cho, Interactions between natural organic matter (NOM) and membranes: Rejection and fouling. Water Sci. Technol., 40(9), 131-139 (1999).
10. Becker, W.C. and C.R. O'Melia, Ozone, oxalic acid, and organic matter molecular weight - Effects on coagulation. Ozone-Sci. Eng., 18(4), 311-324 (1996).
11. Dennett, K. E., A. Amirtharajah, T.F. Moran and J.P. Gould, Coagulation: its effect on organic matter. J. Am. Water Works Ass., 88(4) , 129-142 (1996).
12. Buchanan W., F. Roddick, N. Porter and M. Drikas, Fractionation of UV and VUV pretreated natural organic matter from drinking water. Environ. Sci. Technol., 39(12), 4647-4654 (2005).
13. Marhaba, T.F. and D. Van, The variation of mass and disinfection by-product formation potential of dissolved organic matter fractions along a conventional surface water treatment plant. J. Hazard. Mater., 74(3), 133-147 (2000).
14. Marhaba, T.F., D. Van and R.L. Lippincott, Changes in NOM fractionation through treatment: A comparison of ozonation and chlorination. Ozone-Sci. Eng., 22(3), 249-266 (2000).
15. Świetlik, J., A. Dąbrowska, U. Raczyk-Stanisławiak and J. Nawrocki, Reactivity of natural organic matter fractions with chlorine dioxide and ozone. Water Res., 38(3), 547-558 (2004).
16. Newcombe, G., M. Drikas, A. Assemi and R. Beckett, Influence of characterized natural organic material on activated carbon adsorption: I. Characterization of concentrated reservoir water. Water Res., 31(5), 965-972 (1997).
17. Amy, G., R. Sierka, J. Bedessem, D. Price and L. Tan, Molecular size distributions of dissolved organic matter. J. Am. Water Works Ass., 84(6), 67-75 (1992).
18. Kerc, A., M. Bekbolet and A.M. Saatci, Effects of oxidative treatment techniques on molecular size distribution of humic acids. Water Sci. Technol., 49(4), 7-12 (2004).
19. Müller, M.B. and F.H. Frimmel, A new concept for the fractionation of DOM as a basis for its combined chemical and biological characterization. Water Res., 36(10), 2643-2655 (2002).
20. Barber, L.B., J.A. Leenheer, T.I. Noyes and E.A. Stiles, Nature and transformation of dissolved organic matter in treatment wetlands. Environ. Sci. Technol., 35(24), 4805-4816 (2001).
21. Pedersen, J.A., C.J. Gablelich, C.H. Lin and I.H. Suffet, Aeration effects on the partitioning of a PCB to anoxic estuarine sediment pore water dissolved organic matter. Environ. Sci. Technol., 33(9), 1388-1397 (1999).
22. Leenheer, J.A., Comprehensive approach to preparative isolation and fractionation of dissolved organic carbon from natural and wastewaters. Environ. Sci. Technol., 15(5), 578-

587 (1981).
23. Rosario-Ortiz, F.L., S. Snyder and I.H. Suffet, Characterization of the polarity of natural organic matter under ambient conditions by the polarity rapid assessment method (PRAM). Environ. Sci. Technol., 41(14), 4895-4900 (2007).
24. Rosario-Ortiz, F.L., H.A. Al-Samarrai, K. Kozawa, F.W. Gerringer, C.J. Gabelich and I.H. Suffet, Characterization of the changes in polarity of natural organic matter using solid phase extraction: Introducing the NOM polarity rapid assessment method (NOM-PRAM). Water Sci. Technol.: Water Supply, 4(4), 11-18 (2004).
25. Rosario-Ortiz, F.L., S. Snyder and I.H. Suffet, Characterization of dissolved organic matter in drinking water sources impacted by multiple tributaries. Water Res., 41(18), 4115-4128 (2007).
26. Yan, M., D. Wang, B. Shi, M. Wang and Y. Yan, Effect of pre-ozonation on optimized coagulation of a typical North China source water. Chemosphere, 69(11), 1695-1702 (2007).
27. Galapate, R.P., A.U. Baes and M. Okada, Transformation of dissolved organic matter during ozonation: Effects on trihalomethane formation potential. Water Res., 35(9), 2201-2206 (2001).
28. Owen, D.M., G.L. Amy, Z.K. Chowdhury, R. Paode, G. McCoy and K. Viscosil, NOM characterization and treatability. J. Am. Water Works Ass., 87(1), 46-63 (1995).
29. Griffini,O., M.L. Bao, K. Barbieri, D. Burrini, D. Santianni and F. Pantani, Formation and removal of biodegradable ozonation by-products during ozonation-biofiltration treatment: Pilot-scale evaluation. Ozone-Sci. Eng., 21(1), 79-98 (1999).
30. Gagnon, G.A., S.D.J. Booth, S. Peldszus, D. Mutti, F. Smith and P.M. Huck, Carboxylic acids: formation and removal in full-scale plants. J. Am. Water Works Ass., 89(8), 88-97 (1997).
31. Matilainen, A., N. Lindqvist, S. Korhonen and T. Tuhkanen, Removal of NOM in the different stages of the water treatment process. Environ. Int., 28(6), 457- 465 (2002).
32. Chow, C.W.K., J.A. van Leeuwen, M. Drikas, R. Fabris, K.M. Spark and D.W. Page, The impact of the character of natural organic matter in conventional treatment with alum. Water Sci. Technol., 40(9), 97-104 (1999).
33. American Public Health Association, Standard Methods for the Examination of Water and Wastewater. 20th Ed., American Public Health Association, Washington, DC (1998).
34. Hilderbrand, J.H. and R.L. Scott, The Solubility of Nonelectrolytes. Reinhold, New York (1950).
35. Weishaar, J.L., G.R. Aiken, B.A. Bergamaschi, M.S. Fram, R. Fujii and K. Mopper, Evaluation of specific ultraviolet absorbance as an indicator of the chemical composition and reactivity of dissolved organic matter. Environ. Sci. Technol., 37(20), 4702-4708 (2003).
36. Taylor, J.R., An Introduction to Error Analysis: The Study of Uncertainties in Physical Measurements. Second Edition, University Science Books, Sausalito, CA (1997).
37. Sohn, J., G. Amy and Y. Yoon, Process-train profiles of NOM through a drinking water treatment plant. J. Am. Water Works Ass., 99(6), 145-153 (2007).
38. Chiang, P.C., E.E. Chang and C.H. Liang, NOM characteristics and treatabilities of ozonation processes. Chemosphere, 46(6), 929-936 (2002).

Discussions of this paper may appear in the discussion section of a future issue. All discussions should be submitted to the Editor-in-Chief within six months of publication.

Manuscript Received: November 23, 2007
Revision Received: April 30, 2008
and Accepted: May 31, 2008